Evaluating the potential of electric thermal storage devices to manage greenhouse peak heating demand in cold climates.

Mathieu Laroche, Danielle Monfet, Katherine D'Avignon
École de technologie supérieure, Montréal, Canada

Abstract

To reduce peak demand for electric heating in small-scale greenhouses, thermal energy storage (TES) devices can be implemented. Studies that have explored the potential of TES in greenhouses have primarily focused on seasonal storage. This paper evaluated the daily load-shifting capabilities of a central electric thermal storage (ETS) device using EnergyPlus. Simulations were run using a regression-based model of a hydronic ETS device, coupled with a calibrated greenhouse energy model, to determine the ETS performance in achieving the desired demand management capabilities under various Quebec climates. This included a design procedure to establish the ETS temperature setpoints for each climate. As a result, the load-shifting solution reduced the greenhouse heating demand by 74 % to 77 % during peak hours for four different Quebec climates.

Introduction

Electricity in Quebec is primarily produced from very low-carbon renewable sources, mainly hydroelectric dams, managed exclusively by Hydro-Québec. Today's increasing power demand leads to unprecedented grid pressure, to the point where Hydro-Québec announced the imminent saturation of its installed capacity (Baril, 2022). For greenhouse installations, this represents a challenge for electrification since the main source of heating is currently fossil fuel (natural gas, propane, etc.) (Pelletier & Godbout, 2017). To encourage the electrification of the sector, Hydro-Québec offers a reduced rate for the electricity used for crop lighting and production space heating, which becomes interruptible during cold weather events (Hydro-Québec, 2024a). Some solutions have been explored, such as dual energy systems, where electricity is prioritized, and natural gas is used to supply higher demand on colder days (Hydro-Québec, 2024b). Thermal energy storage (TES) stands as a solution to mitigate the impact of the energy demand of a greenhouse on the power grid by reducing hourly variations and shifting energy consumption away from peak periods. Several studies that explored the potential of TES in greenhouses focussed on seasonal storage and phase change materials in structural components of the greenhouse (Maheux et al., 2023; Gorjian et al., 2021). Such installations require large quantities of storage medium, such as rock beds and aquifers, affect structural components, and can hardly be retrofitted, limiting their widespread adoption. Smaller TES devices, namely electric thermal storage (ETS) devices, are currently available on the market and could avoid these setbacks. They have a small footprint and offer a short charge/discharge cycle that allows for daily peak management, unlike seasonal storage solutions. This paper aims to assess the performance of ETS for greenhouse demand management under various Quebec climates using EnergyPlus (Crawley et al., 2001). First, the demand profile of a typical small-scale greenhouse is generated using a calibrated model. The greenhouse model is then coupled with a regression-based model of a hydronic ETS device. A design procedure is presented to establish the ETS temperature setpoints for a load-shifting strategy to reduce the electric demand during peak hours. Finally, indicators are used to characterize the performance of the energy management strategy in each climate.

Model description

The proposed approach is based on coupling two models: a greenhouse model and a hydronic ETS model.

Greenhouse model

The greenhouse model was developed by Léveillé-Guillemette (2019) and represented a gas-heated, small-scale gothic arch greenhouse of 116.15 m^2, typically found in Quebec, as shown in Figure 1. The steel frame greenhouse envelope cover is mainly made of inflated double-layer polyethylene. Its end walls are made of 4mm thick, rigid polycarbonate panels. Its floor rests on gravel while the structure is anchored in concrete footing. The infiltration rate was set to 0.6 ACH, as recommended by ASHRAE (2015). Additionally, sensible and latent heat gain/loss induced by tomato crops having a Leaf Area Index (LAI) of 2.1 are included (Talbot & Monfet, 2018).

The greenhouse is equipped with a 35 kW natural gas unit heater. Four 50 W fans, attached to the frame's joists, continuously ensure air mixing. Heating setpoints are fixed at 20°C from 6:00 to 21:00 and 16°C from 21:00 to 6:00 to maintain crop growth and fruit production (Turcotte & Larouche, 2015). Humidity is maintained between 60% and 80% using a direct expansion dehumidifier. The unit gas heater is always available, except during summer months,

from May 1st to August 31st, when it is limited to night-time operation. To avoid overheating, a 7.5 m² roof vent and two 15 m² side vents can be manually opened to ensure greenhouse cooling when the indoor temperature reaches 28°C. The model was calibrated using measured data from an existing greenhouse located in Montreal, as described in Léveillé-Guillemette & Monfet (2018).

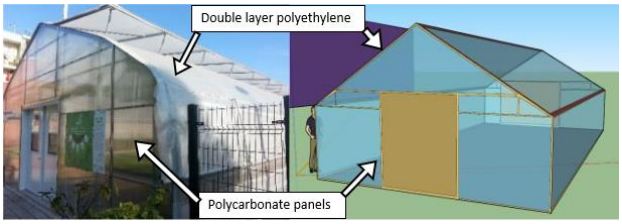

Figure 1: Representation of the greenhouse, adapted from Léveillé-Guillemette & Monfet (2018)

Since the thermal storage device considered for this study requires a hydronic system to deliver its heat, the baseline model is created by replacing the natural gas unit heater with a constant air volume (CAV) hydronic fan coil unit in the original model. Figure 2 illustrates the heating system of the baseline model with the hot water produced using an electric boiler. The modifications are implemented using the OpenStudio v.3.7.0 interface (Guglielmetti et al., 2011) and the equipment parameters listed in Table 1.

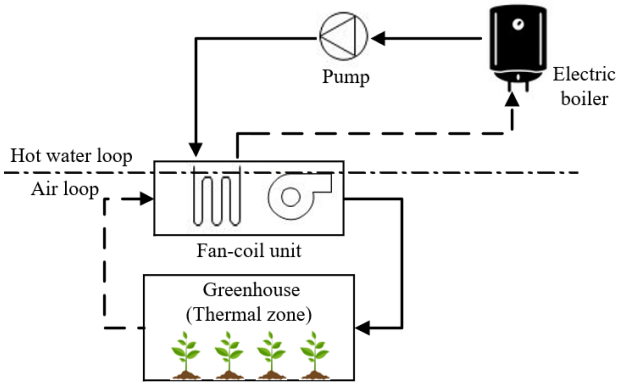

Figure 2: Diagram of the heating system for the baseline model

For this baseline model, the heating season is from September to April. Figure 3 illustrates three daily greenhouse profiles corresponding to different daily average outdoor temperature ranges and the distribution of peak heating demand (P_{heat}) throughout the heating season in the Montreal climate. For all three profiles, there is a similar increase in peak demand from 6:00 to 7:00 after the setpoint shifts from 16°C to 20°C. There is also an important drop in demand during the daytime, where solar gains meet most of the heating demand. The daily heating profiles of the greenhouse exhibit similar patterns throughout the heating season, which aids in the development of energy management strategies. The distribution in peak demand (Figure 3A), which can reach 24 kW in Montreal, also reaches its maximum in the morning following the setpoint change.

Table 1: Description of the heating system for the baseline model.

Name of equipment	Description	Characteristics
Hot water loop equipment		
Boiler: HotWater	Setpoint modulated electric water boiler	Capacity: 35.57 kW
Pump: Const. speed	Constant speed pump	Rated power: 246 W Pump head: 250 Pa
Coil: Heating: Water	Heating coil, hot water side	Inlet HW temp: 45°C Out. HW temp: 40°C Water flow: Autosize
Zone equipment		
CV Unit Heater HW	Constant volume fan-coil unit	Air in temp: 16.6°C Air out temp: 40°C Capacity: Autosize Max flow: Autosize Pressure rise: 250 Pa

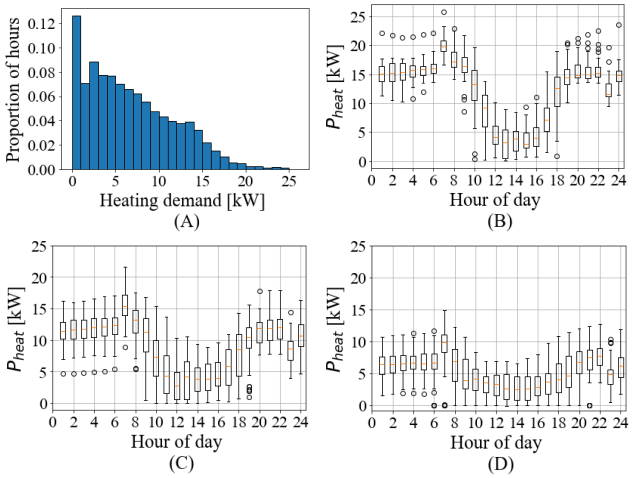

Figure 3: Baseline greenhouse heating demand in Montreal: hourly demand distribution (A) and hourly heating demand for daily average outdoor temperature ranges of (B) -20°C to -10°C, (C) -10°C to 0°C, (D) 0°C to 10°C

Electric thermal storage model

The ETS model used is a regression-based characterization of a central hydronic ETS device developed by Younes et al. (2023). The model is based on a Steffes ThermElect 9180 ETS device, composed of three brick cores of 96 bricks, which can reach up to 760°C and store up to 440 kWh of heat (Steffes, n.d.a). Figure 4 shows a sectional view of the device. The heat is recuperated using a variable-speed fan that circulates the air over the hot bricks. This hot air then passes through an air-liquid heat exchanger to transfer the heat to the hot water (HW) heating loop. The model has been made into an OpenStudio 'Measure' and can be implemented in any existing EnergyPlus model.

For its implementation, a series of schedules and setpoints must be specified. First, the operating schedule must be determined to dictate whether or not the unit can be charged and/or discharged at any given moment. A load-shifting strategy will be implemented, allowing the ETS to charge during off-peak hours and discharge during peak hours. Second, the average brick core temperature ($\bar{T}_b$) is controlled using a user-defined setpoint ramp based on the outdoor temperature, as illustrated in Figure 8. The design procedure to establish the setpoints and schedules is detailed in the Method section.

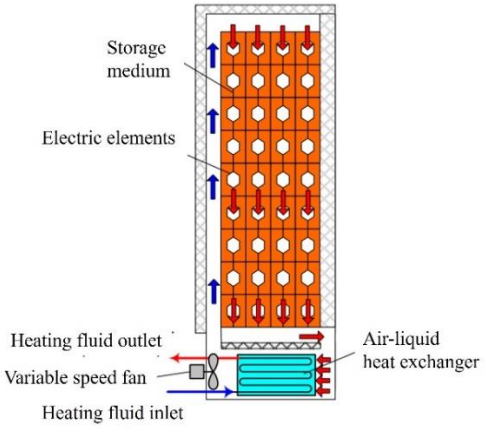

Figure 4: Sectional view of the ETS device, Moreau (2010)

The model definition in Younes et al. (2024) characterizes the three brick cores as a single lumped-capacitance, with an average brick core temperature ($\bar{T}_b$). The model assumes that ($\bar{T}_b$) dictates both the hot water temperature rise achievable by the ETS unit ($\Delta T_{HW,ETS}$) and the amount of energy stored (Q_{sto}) as defined by equations (1) and (2).

$$\Delta T_{HW,ETS}(t) = T_{HW,in}(t) - T_{HW,out}(t) = p_1 \cdot \bar{T}_b{}^2 + p_2 \cdot \bar{T}_b + p_3 \quad (1)$$

$$Q_{sto}(t) = M_b \cdot C_{p,b} \cdot (\bar{T}_b(t) - \bar{T}_b(t-1)) \quad (2)$$

The $\Delta T_{HW,ETS}$ can be calculated through a polynomial equation, where p_1, p_2 and p_3 have been defined respectively as -1.05E-05, 0.0232, and -0.188 for the Steffes 9180 unit. Q_{sto} can be defined according to the change in average brick core temperature ($\bar{T}_b$) over time (t) multiplied by the brick mass (M_b) of 2340.5 kg and specific heat ($C_{p,b}$) of 0.92 kJ (kg·K)$^{-1}$.

Method

The proposed procedure starts by analyzing the baseline energy profile and identifying the parameters required to implement the ETS model. The ETS's impact is then assessed using performance indicators calculated from simulation results. The procedure for the greenhouse located in Montreal is detailed. As presented in the results, this procedure has been replicated for three additional climates: Quebec City, Baie-Comeau, and Kuujjuaq.

Baseline profile analysis

The ETS device's control strategy, operating schedule, and temperature setpoints must be established before implementing the ETS model. For the operating schedule, i.e., the charging and discharging schedules, peak demand periods defined by Quebec energy provider Hydro-Québec as 6:00 to 9:00 and 16:00 to 20:00 are used (Hydro-Québec, 2024c). The ETS can charge during off-peak periods, while discharging is limited to peak periods, as shown in Figure 5. Figure 5 presents a typical day's heating demand (P_{heat}) profile for the Montreal greenhouse, where ps represents the time at which the evening peak period begins, i.e., 16:00. Q_{sto} is also shown, representing the required heating energy for each peak period.

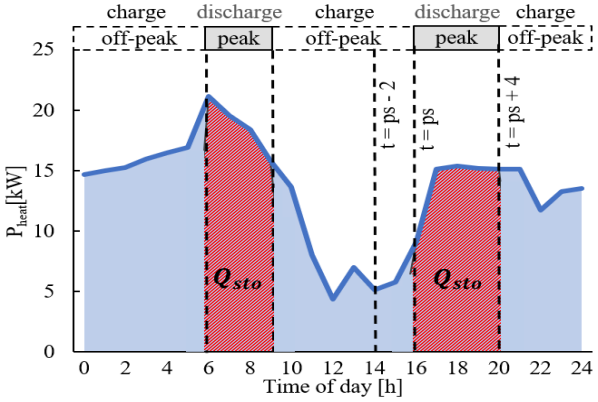

Figure 5: Typical daily heating demand with peak and off-peak periods

A more refined analysis is required to select the device's average brick core temperature setpoint ($\bar{T}_{b,SP}$), which is fixed according to the outdoor air temperature ($T_{O/A}$). This requires analyzing the outdoor temperature profiles against the heating demand of the greenhouse. The minimum ($\bar{T}_{b,SPmin}$) and maximum ($\bar{T}_{b,SPmax}$) values of the $\bar{T}_{b,SP}$ ramp, illustrated on Figure 8, must be adjusted depending on the climate. In this method, observed values are limited to the heating season, from September 1st to April 30th, when the ETS device is active. The procedure to establish $\bar{T}_{b,SP}$ is illustrated in Figure 6.

The first step is to extract each value of hot water temperature rise (ΔT_{HW}) from the simulation results of the baseline case. This value is defined as the difference between the boiler inlet ($T_{HW,in}(t)$) and outlet ($T_{HW,out}(t)$) temperatures. Then, the maximum hot water temperature rises ($\Delta T_{HW,max}$) of each evening peak period is identified. The values of $\Delta T_{HW,max}$ are inputted to equation (1) in lieu of $\Delta T_{HW,ETS}$. Solving equation (1) for $\bar{T}_b$ allows the identification of the minimum brick temperature ($\bar{T}_{b,min}$) required to meet the maximum heating demand of each evening peak.

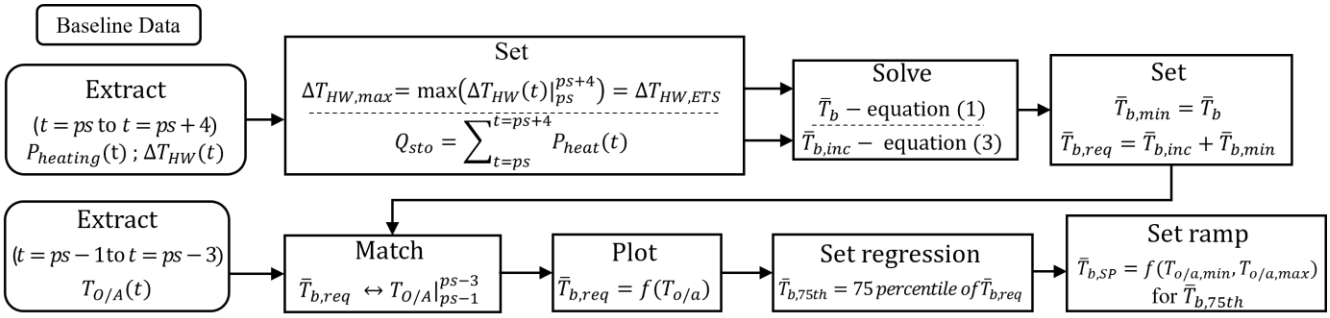

Figure 6: Procedure using the baseline data to establish the brick setpoint temperature

In parallel, the required stored energy (Q_{sto}) is calculated for each evening peak period over the heating season. This is done by summing the hourly heating demand over the peak period ($\sum_{ps}^{ps+4} P_{heat}$) from the baseline case simulation results. Q_{sto} is then input in equation (3), which is a modified version of equation (2), where the value of Q_{sto} is tied to a single value of the increase in brick temperature ($\bar{T}_{b,inc}$).

$$\bar{T}_{b,inc} = \bar{T}_b(t) - \bar{T}_b(t-1) = \frac{Q_{sto}}{M_b \cdot C_{p,b}} \qquad (3)$$

Solving equation 3 allows to define $\bar{T}_{b,inc}$, the brick temperature required to supply Q_{sto} over each evening peak. Once the minimum brick temperature ($\bar{T}_{b,min}$) and brick temperature increase ($\bar{T}_{b,inc}$) are identified, both values are added to define the required brick temperature ($\bar{T}_{b,req}$) for each evening peak period over the heating season. Each value of $\bar{T}_{b,req}$ can be paired with the outdoor temperatures from the 3 hours prior to its corresponding peak period ($T_{O/A}|_{ps-1}^{ps-3}$). This accounts for the interval between the charging and discharging periods. Hence, when the ETS device reads the outdoor temperatures prior to the peak period, the control logic must require that it charges to $\bar{T}_{b,req}$, so the setpoint is reached before the peak period begins. $\bar{T}_{b,req}$ is plotted as a function of $T_{O/A}$. This relation is shown in Figure 7 for the Montreal climate, through a boxplot with 1°C range bins to account for measurement uncertainties, solar gains, and wind variations.

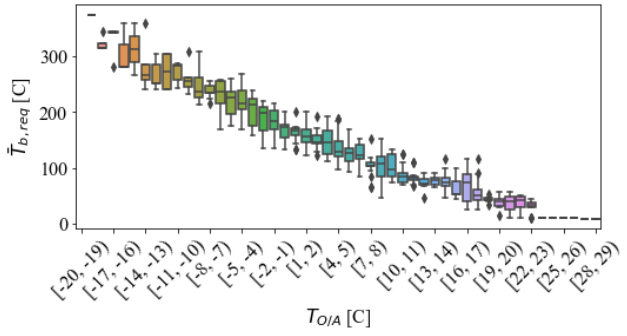

Figure 7: Required brick temperature ($\bar{T}_{b,req}$) as a function of outdoor temperature ($T_{O/A}$) for the Montreal climate

A regression resulting from this boxplot allows to draw a ramp, defining the brick temperature setpoint ($\bar{T}_{b,SP}$) as a function of $T_{O/A}$. However, one additional step is required to establish a linear regression that does not lead to under-charging of the ETS. This step is included since a linear regression representing the entire processed data as a "line of best fit" would generally align closer to the midpoint of the multiple setpoint pairs for each temperature bin. Instead, for each bin of the boxplot, the 75th percentile of $\bar{T}_{b,req}$ is paired with the highest $T_{O/A}$ value within the bin. The 75th percentile is chosen assuming it will limit overcharging while allowing the ETS to keep a high enough brick temperature to meet most of the peak's heating needs. Figure 8 illustrates, as an example for Montreal, a line of best fit, representing the relationship between the 75th percentile values of $\bar{T}_{b,req}$ ($\bar{T}_{b,75th}$) and the highest $T_{O/A}$ of each bin. A brick temperature of 93°C is identified by Steffes (n.d.b) as the minimum temperature for effective heat output; it is used as the minimum setpoint average brick core temperature ($\bar{T}_{b,SPmin}$). Consequently, the maximum operating outdoor temperature ($T_{O/A,max}$) is the value which warrants a brick temperature of 93°C. The minimum operating outdoor temperature ($T_{O/A,min}$) is defined according to when the required brick temperature either plateaus or becomes unstable, e.g., -18.9°C for Montreal (Figure 8). The maximum setpoint average brick core temperature ($\bar{T}_{b,SPmax}$) is defined using the equation for $\bar{T}_{b,75th}$ with $T_{O/A,min}$ as an input.

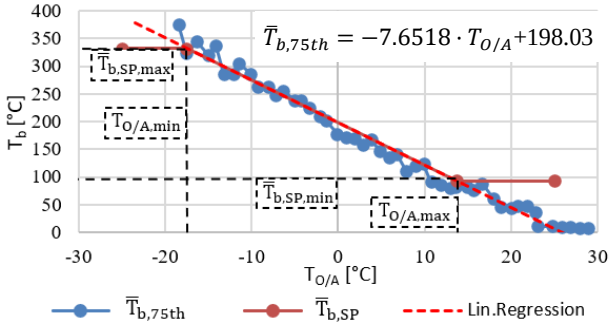

Figure 8: Regression of $\bar{T}_{b,75th}$ as a function of $T_{O/A}$

The ETS device's setpoint ramp is then implemented by specifying the following temperatures in the ETS model: $T_{O/A,min}$, $T_{O/A,max}$, $\bar{T}_{b,SPmin}$, $\bar{T}_{b,SPmax}$.

Greenhouse-ETS model

The Greenhouse-ETS model is similar to the baseline model, except for adding the ETS device upstream of the boiler in the hot water loop, as shown in Figure 9. The main change is in the control sequence for the demand management strategy. The load-shifting strategy uses the previously defined schedules and brick temperature setpoints. During peak periods, priority is given to the ETS device, followed by the auxiliary equipment, which is used to cover any unmet demand. In off-peak periods, the ETS device can only charge while the auxiliary heating source, an electric boiler, meets the greenhouse's total heating demand. The maximum inlet power of the ETS device is set to 15 kW to limit the charging rate and to ensure that the greenhouse's demand remains within the maximum power output allocated by the utility company (Hydro-Québec, 2024b). In an ideal scenario, the electricity consumption of heating equipment would remain null throughout the peak periods.

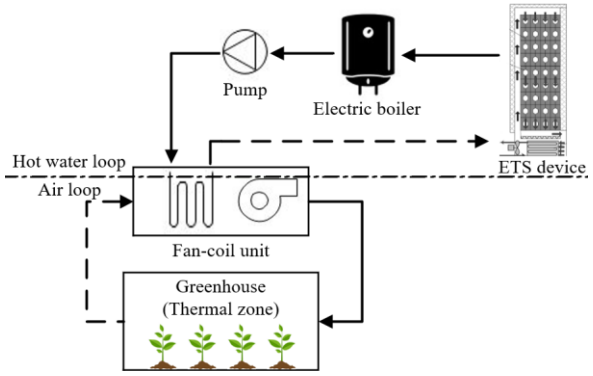

Figure 9: Diagram of Greenhouse-ETS heating system model

Performance indicators

The performance of the ETS storage scenario can be assessed using different indicators (Luo et al., 2017; Morovat et al., 2021), allowing the performance to be characterized over daily to annual periods. In this paper, a combination of three indicators is used to determine the energy management capabilities of the ETS device. Two load-shifting performance indicators have been proposed by Zhang, Saloux, and Candanedo (2024): the energy flexibility (Ef) and the energy rebound (E_{rb}) as defined respectively by equations (4) and (5). The Ef represents the total energy removed from the baseline case during a peak period, from time $t = ps$ to time $t = ps + i$ where i is the number of hours in the observed peak period. In contrast, the E_{rb} documents the total energy added to the baseline case before and after the peak event. To do so, the difference in power demand between the baseline scenario (P_{ref}) and the load-shifting scenario (P_{ls}) is integrated over a period of $a/2$, where a is the number of hours between subsequent peak periods.

$$Ef = \int_{ps}^{ps+i} (P_{ls} - P_{ref})dt \quad (4)$$

$$E_{rb} = \int_{-\frac{a}{2}}^{ps} (P_{ls} - P_{ref})dt + \int_{ps+i}^{ps+i+\frac{a}{2}} (P_{ls} - P_{ref})dt \quad (5)$$

Zhang, Saloux, and Candanedo (2024) proposed an additional indicator, the energy efficiency (ηf) of the load-shifting solution, as defined by equation (6). Using both Ef and E_{rb},this indicator shows the fraction of displaced energy compared to the required energy input to the storage.

$$\eta f = \left|\frac{E_f}{E_{rb}}\right| \quad (6)$$

Results

Using the OpenStudio interface and CWEC weather files (Natural Resources Canada, 2023), the energy profiles were generated by simulating the baseline greenhouse model in four climates: Montreal, Quebec City, Baie-Comeau, and Kuujjuaq. These profiles were analyzed to determine the ETS device's temperature setpoints for each climate as a function of outdoor temperature, as shown in Table 2. The yearly energy profiles of the Greenhouse-ETS model were then generated for the four climates equipped with the same ETS device using the implemented setpoints.

Table 2: Brick setpoints ramp values for each climate (°C)

Climate	$\bar{T}_{b,SPmin}$	$T_{O/A,max}$	$\bar{T}_{b,SPmax}$	$T_{O/A,min}$
Montreal	93.0	13.7	332.1	-17.5
Quebec City	93.0	13.9	317.2	-14.6
Baie-Comeau	93.0	13.1	353.3	-16.7
Kuujjuaq	93.0	12.0	403.7	-25.0

Impact of ETS on energy profiles

Figure 10 illustrates the impact of using the ETS on the energy profile for January 21st in each climate, which represents an average heating demand profile for cooler temperatures, as illustrated in Figure 3(B). The implemented strategy aimed to reduce the demand during both daily peak periods, during which energy prices increase. The results show a reduction of 77% of the demand during peak periods, accounting for the entire on-peak heating demand for that day in Montreal's climate. In colder climates, the control strategy and setpoints defined using the 75th percentile method enabled the displacement of nearly all heating demand during peak periods to off-peak periods in cold weather. However, the strategy also leads to a higher overall demand from the greenhouse in each climate.

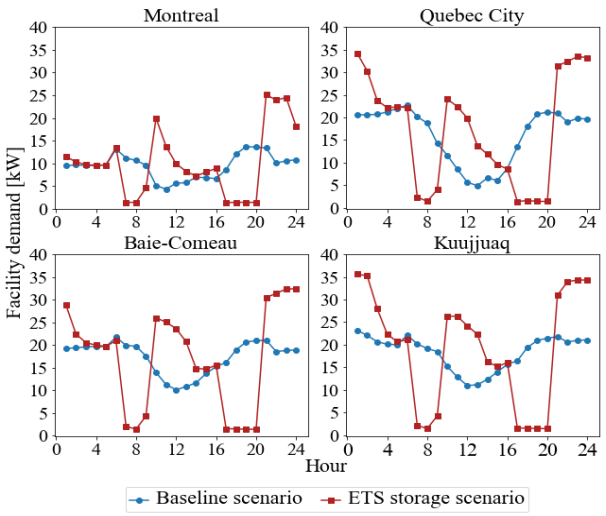

Figure 10: Profiles from Baseline and ETS scenario in the 4 climates for January 21st

ETS performance analysis

The performance of the ETS storage scenario is assessed using three indicators computed over the heating season, from September 1st to April 30th.

Table 3 includes the maximum heating demand ($P_{heat,max}$) and the boiler consumption during all peak periods (E_{Boiler}) for the baseline and the Greenhouse-ETS cases over the heating season as well as the values of Ef, E_{rb}, and ηf. Since the energy efficiency (ηf) combines the indicators for energy flexibility and rebound, it is also analyzed on a monthly basis, as illustrated in Figure 11.

By comparing the monthly values of ηf shown in Figure 11, a trend can be observed where the colder months make better use of the stored energy. This is explained by the fact that the energy losses of the device inside the greenhouse lead to reduced boiler demand to maintain the setpoint temperature during off-peak periods. Slight inefficiencies arise when the weather is mild enough not to require off-peak boiler operation. At those times, the ETS heat losses maintain the indoor temperature between the heating/cooling dead band temperatures. However, during milder weather, such as in September, energy losses occasionally led to overheating in the greenhouse. This triggered the opening of the roof vents, causing heat to escape outside the greenhouse, resulting in a net energy loss. As a result, colder climates tend to perform better in this regard when using the same schedule across all climates.

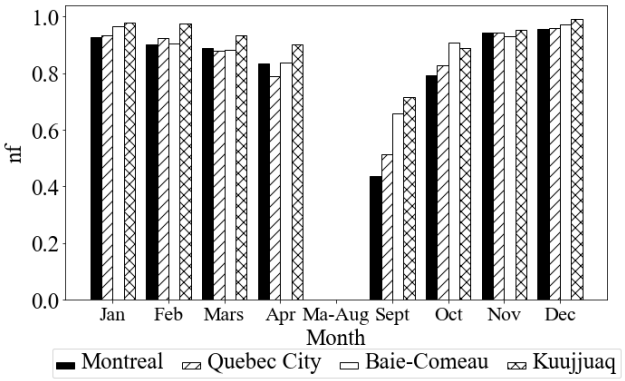

Figure 11: Monthly ηf values in every climate

Discussion

The results show that, even in the case of a small-scale greenhouse, the annual efficiency of the load-shifting solution is higher than 89% while allowing the displacement of around 96% of the greenhouse's heating energy use during peak periods. Despite using the ETS, there is still some use of the boiler during peak periods, mainly explained by some undercharging of the device. The maximum peak demand is reduced by 16.8 kW to 20 kW compared to the baseline case, depending on the climate. Colder climates experienced more significant benefits, with annual efficiency reaching 94.6%. Analysis of the simulation results supported identifying several factors that affect the ETS storage scenario's performance. For example, the recommended minimum brick core temperature of 93°C must be considered when enabling the ETS device, as it impacts its operating schedule.

Critical inefficiencies were noted in September caused by overcharging of the device. Another cause of inefficiency in mild weather is the device's heat losses, influencing the greenhouse's indoor air temperature. This influx of heat can lead to overheating of the greenhouse in milder weather, requiring cooling to maintain the temperature setpoint. Hence, ETS usage should be limited to periods where outdoor temperatures warrant changes in brick core temperature.

Table 3: Performance indicators over the heating season

Climate	$HDD_{18°C}$	Baseline		Greenhouse-ETS		Ef [kWh]	E_{rb} [kWh]	ηf
		$P_{heat,max}$ [kW]	E_{Boiler} [kWh]	$P_{heat,max}$ [kW]	E_{Boiler} [kWh]			
Montreal	4191	22.7	11 201	5.8	29.1	-10 748	11 988	89.7%
Quebec City	4842	23.0	12 358	5.9	39.4	-11 881	13 265	89.6%
Baie-Comeau	5487	24.2	13 997	5.8	42	-13 517	14 738	91.7%
Kuujjuaq	7984	25.7	18 777	6.0	94.1	-18 211	19 254	94.6%

Results showed that for colder periods, from November to February, the efficiency of the storage scenario is mostly consistent across the four studied climates. Efficiencies recorded for September and October were considerably higher in Kuujjuaq, reaching 71.4% and 88.7% compared to Montreal's 43.7% and 79.3% for the same months.

Therefore, the length of the heating season should be adjusted according to the climate and be included as an additional step as part of the load-shifting design procedure. The simulations also revealed that the design procedure used to identify valid ETS brick temperature setpoints can be challenging and requires an in-depth analysis of the greenhouse's profile. Arbitrary decisions made in this paper, such as the choice of the percentile on which to base the brick temperature setpoint ramp, can significantly affect the efficiency of the storage solution. Additional testing would be required to establish the optimal percentile value to determine the ETS setpoint temperatures. The low boiler consumption during peak periods suggests that lowering the brick temperature setpoint could be feasible. Even in colder climates, the 75th percentile appears to be a rather conservative approach.

Another variable that has not been thoroughly studied is the morning and evening peak weather patterns. The method presented was based on the hypothesis that morning peak periods, lasting for 3 hours, require less energy than the evening peak, which lasts 4 hours. However, heating demand is typically higher in the morning due to both the lower outdoor air temperatures and the transition from the nighttime indoor temperature setpoint (16°C) to the daytime temperature setpoint (20°C). The higher demand may be offset by the shorter duration of the peak period. Focus was set on the evening peak data to establish the brick temperature setpoint ramp since typical weather patterns show that outdoor temperatures are higher during daytime than nighttime. Hence, the ETS device would be tuned in such a way that enough energy would be stored even when the device is subjected to higher outdoor temperatures. Analyzing both peak period needs may be required to fix a reliable setpoint ramp.

While the results of the simulations are encouraging, it is essential to point out that important aspects of thermal storage are overlooked. The strategy did not consider the accuracy of the ETS device's temperature control abilities. The hot water temperature difference through the ETS device ($\Delta T_{HW,ETS}(t)$), sometimes as low as 0.07°C, cannot be accurately controlled in a real application. Since the model from Younes et al. (2023) can accurately deliver energy even in such low-temperature rise situations, it has been possible to test the solution in periods that would have been too mild to ensure adequate control. Furthermore, the ETS device modelled, rated for an output of up to 80 kW, is oversized for the heating demand of the greenhouse. No other hydronic ETS numerical models with smaller capacities were found in the literature. They may be more suitable for Quebec's greenhouse needs if they become available. With this in mind, an ETS charging bound was arbitrarily set to limit the increase of the off-peak demand. The brick temperature setpoint ramp also allowed to scale down the storage capacity for the simulations. A detailed cost analysis would be required to define the optimal charging power allowed for the ETS device.

Another limiting factor in the Greenhouse-ETS model is the use of instantaneous outdoor temperatures instead of weather forecasts, which influences thermal storage efficiency. Using weather forecasts could further limit overcharging and allow the use of a higher percentile value when defining the setpoint ramp temperatures, covering a wider range of heating peaks while limiting the drawback of overcharging. Recent studies successfully controlled thermal storage solutions in simulations and applications using weather forecasts (Cesari et al., 2022; Kuosa et al., 2022).

Conclusion

By using the regression model from Younes et al. (2023), it was possible to implement an ETS device into a typical small-scale greenhouse model. Using performance indicators and testing the strategy in different climates provided insight into the behaviour and cross-effects of the ETS device. Colder climates benefitted more from the device, while the strategy caused non-negligible energy loss in milder weather. Despite the non-optimal control, high solution efficiencies, above 89%, were noted for the studied climates. The device effectively allowed the maximum peak period demand to be reduced by at least 17 kW compared to the baseline scenario. A design procedure allowed the definition of the thermal storage temperature setpoint. This procedure required arbitrary decisions, and a few variables were explored. Further evaluation would be required to define the set-point ramp better and adapt it to each climate's weather pattern. Weather forecasts would also allow for a smaller design margin and limit the overcharging, increasing efficiency in milder months.

Acknowledgments

While preparing this work, the authors used ChatGPT 3.5 to generate scripts to enhance data presentation and improve the language and readability of a few sentences (less than 10% of the text). After using this tool/service, the authors reviewed and edited the content as needed and took full responsibility for the publication's content. This work was supported by NSERC Graduate Scholarships – Master's program for the first co-author.

References

Baril, H. 2022. Hydro-Québec revoit encore à la hausse ses besoins en électricité. *La Presse*. Available at: https://bit.ly/3wpPgUQ [Accessed February 6, 2024].

Belzile, P., Kajl, S., Rousse, D., & Dutil, Y. 2012. Electrical thermal storage optimization for demand side management.

Cesari, S., Emmi, G., & Bottarelli, M. 2022. A weather forecast-based control for the improvement of PCM enhanced radiant floors. *ATEN* 206.: 10.1016/j.applthermaleng.2022.118119

Crawley, D. B. et al. (2001). "EnergyPlus: Creating a new-generation building energy simulation program." Energy and Buildings 33(4): 319-331.

Gorjian, S., Ebadi, H., Najafi, G., Singh Chandel, S., & Yildizhan, H. 2021. Recent advances in net-zero energy greenhouses and adapted thermal energy storage systems. *Sustainable Energy Technologies and Assessments* 43. 10.1016/j.seta.2020.100940.

Guglielmetti, R., D. Macumber and N. Long (2011). Openstudio: An open source integrated analysis platform. BS 2011, Sydney, NSW, Australia.

Hydro-Québec a. Rate option for raising crops. Available at: https://www.hydroquebec.com/residential/customer-space/rates/additional-electricity-option-crops.html [Accessed May 8, 2024].

Hydro-Québec b. Rate DT – Dual Energy for residential and agricultural customers. Available at: https://www.hydroquebec.com/residential/customer-space/rates/rate-dt.html [Accessed February 6, 2024].

Hydro-Québec c. Save during winter peak periods. Available at: https://www.hydroquebec.com/residential/energy-wise/saving-during-peak-periods/index.html [Accessed Mars 15, 2024].

Kuosa, M. et al. 2022. Optimisation of district heating production by utilising the storage capacity of a district heating network on the basis of weather forecasts. *Results in Engineering* 13 10.1016/j.rineng.2021.100318

Léveillé-Guillemette, F. 2019. *Évaluation des impacts énergétiques et environnementaux de différents modes d'agriculture urbaine en environnement contrôlé*. Montréal, QC, Canada: École de technologie supérieure.

Léveillé-Guillemette, F., & Monfet, D. 2018. Calibration d'un modèle énergétique et analyse économique de mesures de conservation d'énergie d'une serre communautaire à Montréal. eSim2018, QC, Canada.

Luo, X., Hong, T., Chen, Y., & Piette, M.A. 2017. Electric load shape benchmarking for small- and medium-sized commercial buildings. *Applied Energy* 204: p.715–725.

Maheux, T., Monfet, D., Gibout, S., & Haillot, D. 2023. Modélisation d'une serre couplée à un système de stockage thermique : développement d'un modèle et étude de validité. SFT 2023, Reims, France.

Moreau, Alain. 2010. « Un nouvel appareil de chauffage avec accumulation de chaleur pour les secteurs commercial et institutionnel ». *CIFEM*. (Saly, Sénégal, 17-19 mai 2010), sous la dir. de d'Hydro-Québec, Institut de recherche, p. ART-3-153.

Morovat, N., Agustín Candanedo, J., & K Athienitis, A. 2021. Energy flexibility quantification with integrated heat pump, floor heating system, and thermal storage in a school building. BS 2011, Sydney, NSW, Australia..

Natural Resources Canada. 2023. Canadian Weather Year for Energy Calculation (CWEC). Available at: https://open.canada.ca/data/en/dataset/55438acb-aa67-407a-9fdb-1cb21eb24e28 [Accessed March 21, 2024].

Pelletier, F., & Godbout, S. 2017. *Consommation d'énergie et émissions de gaz à effet de serre en production serricole au Québec*. Longueuil, Québec: IRDA.

Steffes. n.d. a Technical Data Sheet 9100 ThermElect Hydronic.

Steffes. n.d. b MASTER SUPPLEMENTAL INSTALLER'S GUIDE for Comfort Plus Commercial and ThermElect Models: 6100, 7100, 8100 and 9100 Series - V8.

Talbot, M.-H., & Monfet, D. 2018. *Impact des plantes sur les charges d'un espace d'agriculture intégré au bâtiment : Implantation d'un modèle de plantes*. eSim2018, QC, Canada.

Turcotte, G., & Larouche, R. 2015. Production de la tomate deserre au Québec (guide technique). Available at: https://www.agrireseau.net/Legumesdeserre/documents/95590/production-de-la-tomate-de-serre-au-quebec-guide-technique [Accessed January 10, 2024].

Yang, D. et al. 2022. A Flexibility Assessment Method of Thermal Storage Electric Heating Load Clusters. In *2022 IEEE 6th Conference on Energy Internet and Energy System Integration (EI2)*, 538–542

Younes, H. E., D'Avignon, K. et Laurencelle, F. (2023) « ltsb-étsmtl/ETS-Openstudio-Measure ». Zenodo. doi: 10.5281/zenodo.10215082.

Younes, H. E., Laurencelle, F. & D'Avignon, K. (2024). Implementing Thermal Electric Storage in EnergyPlus through an OpenStudio Measure. eSIM 2024, Edmonton, Canada

Zhang, K., Saloux, E., & Candanedo, J. 2023. Enhancing Energy Flexibility of Building Clusters Via Supervisory Room Temperature Control: Quantification and Evaluation of Benefits. Available at: https://papers.ssrn.com/abstract=4566520 [Accessed December 11, 2023].